Monthly Notices
of the
ROYAL ASTRONOMICAL SOCIETY

MNRASL **429,** L15–L19 (2013) doi:10.1093/mnrasl/sls014

Systematic variation of the stellar initial mass function with velocity dispersion in early-type galaxies

Ignacio Ferreras,[1⋆] Francesco La Barbera,[2] Ignacio G. de la Rosa,[3,4] Alexandre Vazdekis,[3,4] Reinaldo R. de Carvalho,[5] Jesús Falcón-Barroso[3,4] and Elena Ricciardelli[6]

[1]*Mullard Space Science Laboratory, University College London, Holmbury St Mary, Dorking, Surrey RH5 6NT*
[2]*INAF-Osservatorio Astronomico di Capodimonte, I-80131 Napoli, Italy*
[3]*Instituto de Astrofísica de Canarias, C/ Vía Láctea s/n, La Laguna, E-38200 La Laguna, Tenerife, Spain*
[4]*Departamento de Astrofísica, Universidad de La Laguna, E-38205 La Laguna, Tenerife, Spain*
[5]*Instituto Nacional de Pesquisas Espaciais/MCT, S.J. dos Campos, SP 12227-010, Brazil*
[6]*Departament d'Astronomia i Astrofisica, Universitat de Valencia, C/Dr Moliner 50, E-46100 Burjassot, Valencia, Spain*

Accepted 2012 October 11. Received 2012 October 10; in original form 2012 August 15

ABSTRACT

An essential component of galaxy formation theory is the stellar initial mass function (IMF) that describes the parent distribution of stellar mass in star-forming regions. We present observational evidence in a sample of early-type galaxies (ETGs) of a tight correlation between central velocity dispersion and the strength of several absorption features sensitive to the presence of low-mass stars. Our sample comprises ∼40 000 ETGs from the Spheroids Panchromatic Investigation in Different Environmental Regions survey ($z \lesssim 0.1$). The data – extracted from the Sloan Digital Sky Survey – are combined, rejecting both noisy data, and spectra with contamination from telluric lines, resulting in a set of 18 stacked spectra at high signal-to-noise ratio (S/N $\gtrsim 400\,\text{Å}^{-1}$). A combined analysis of IMF-sensitive line strengths and spectral fitting is performed with the latest state-of-the-art population synthesis models (an extended version of the MILES models). A significant trend is found between IMF slope and velocity dispersion, towards an excess of low-mass stars in the most massive galaxies. Although we emphasize that accurate values of the IMF slope will require a detailed analysis of chemical composition (such as [α/Fe] or even individual element abundance ratios), the observed trends suggest that low-mass ETGs are better fitted by a Kroupa-like IMF, whereas massive galaxies require bottom-heavy IMFs, exceeding the Salpeter slope at $\sigma \gtrsim 200\,\text{km s}^{-1}$.

Key words: galaxies: elliptical and lenticular, cD – galaxies: evolution – galaxies: formation – galaxies: fundamental parameters – galaxies: stellar content.

1 INTRODUCTION

The initial mass function (IMF) is defined as the distribution of stellar masses in a single population at the time of birth. It has been usually considered a universal function, partly because of the complexities in obtaining proper observational constraints. The traditional approximation by a single power law (Salpeter 1955) has undergone numerous updates, with more complex functions that include a significant flattening of the slope towards low-mass stars (Miller & Scalo 1979; Scalo 1986; Kroupa 2001; Chabrier 2003). For a recent review on the IMF and its possible variations, see Bastian, Covey & Meyer (2010).

Past analyses based on dynamical modelling favoured Kroupa-like IMFs in early-type galaxies (ETGs; Cappellari et al. 2006). This result was also found with strong gravitational lensing on the bulge of a late-type galaxy (Ferreras et al. 2010). However, the IMF was suspected to depend on galaxy mass, when extending the analysis to more massive systems, as in the dynamical modelling of Thomas et al. (2011b), with galaxy morphology also playing a role (Brewer et al. 2012). Constraining the low-mass portion of the IMF is a challenging task, as faint, low-mass stars do not contribute significantly to the integrated spectrum. The first observational attempts to constrain the low-mass end of the IMF were made by Cohen (1978) and Faber & French (1980), towards the centres of M31 and M32, measuring several spectral features sensitive to the relative contribution of M dwarves and M giants. Later, Carter, Visvanathan & Pickles (1986) extended the study to a sample of massive ETGs, and found

⋆ E-mail: ferreras@star.ucl.ac.uk

that NaI was enhanced, especially in massive galaxies, with strong radial gradients (being most enhanced in the central region). More recently, Cenarro et al. (2003) proposed a relation towards an excess of low-mass stars in massive galaxies, from a study of the Ca II triplet region at ∼8500 Å. Van Dokkum & Conroy (2010) probed two features in the near-infrared (NIR) that are strongly dependent on the fraction of low-mass stars, to find a bottom-heavy IMF in a sample of four Virgo ETGs. This result was recently extended to an additional set of 34 ETGs from the SAURON survey, with similar conclusions (Conroy & Van Dokkum 2012b), favouring the interpretation of a non-universal IMF. An alternative scenario to explain these data would invoke over/underabundances of individual elements (see e.g. Worthey 1998). Bottom-heavy IMFs would imply that massive galaxies observed at high redshift are even more massive than the standard assumption of a Kroupa-like IMF, posing challenging constraints on the physics underlying the conversion of gas into stars during the first stages of galaxy formation. This issue is of special relevance to the standard paradigm of hierarchical galaxy formation, whereby massive galaxies are supposed to grow mainly through the merging of smaller systems, with the growth rate limited by cosmology (see e.g. De Lucia et al. 2006), requiring alternative channels of massive galaxy formation, such as cold accretion (see e.g. Birnboim & Dekel 2003).

Simple theories of star formation suggest a power-law behaviour, with a truncation at the low-mass end, around 0.3 $M_{\odot}$ (Larson 2005; McKee & Ostriker 2007), consistent with some of the most popular IMFs used (Kroupa 2001; Chabrier 2003). However, due to the lack of strong observable tracers in the observed spectra arising from low-mass stars, a robust constraint at the low-mass end of the IMF has remained elusive for years. In addition to the work cited above, more recent evidence has been accumulating (Van Dokkum & Conroy 2010; Smith J, Lucey & Carter 2012; Spiniello et al. 2012), towards the possibility of a non-universal IMF. This hypothesis is further supported by an independent study that made use of detailed dynamical modelling of nearby spheroidal galaxies (Cappellari et al. 2012). Strong gravitational lensing over galaxy scales also hint at bottom-heavy IMFs in massive galaxies (Auger et al. 2010). The implications of a change in the IMF warrant further analysis of this problem.

2 SAMPLE

The hypothesis of a systematic change in the initial stellar mass function with respect to global properties of galaxies, such as mass or luminosity, is optimally tested on samples of galaxies that harbour stellar populations as homogenous as possible, for a clean analysis of the spectra. The Spheroids Panchromatic Investigation in Different Environmental Regions (SPIDER) sample (La Barbera et al. 2010) is optimal for this purpose, as it comprises 39 993 nearby ($0.05 < z < 0.095$) ETGs, in a wide range of masses, from 2×10^{10} to 10^{12} $M_{\odot}$ (dynamical mass; de la Rosa et al. 2012). Spectra of these galaxies were retrieved from the sixth Data Release of the Sloan Digital Sky Survey (SDSS; Abazajian et al. 2009), deredshifted to a common rest frame (with 1 Å binning) and corrected for foreground Galactic extinction (see La Barbera et al. 2010, for details). In order to test variations of the IMF, we assemble 18 stacked spectra spanning over a wide range of central velocity dispersions (σ) between 100 and 320 km s^{-1} in steps of 10 km s^{-1}, except for the two bins for the highest values of σ, where – because of the smaller number of galaxies in the sample – we adopted the range [260,280], and [280,320] km s^{-1} , respectively. We select the sample according to σ, because (i) the underlying stellar populations of ETGs are known to correlate strongly with this observable (Bernardi et al. 2005) and (ii) the spectral analysis depends sensitively on velocity dispersion, as a higher σ introduces an effectively lower spectral resolution, an issue that we take into account for a consistent comparison (see below).

Given the redshift range of the SPIDER sample, the 3 arcsec diameter of the SDSS fibres maps the central ∼2–3.5 h^{-1} kpc. For each bin, we perform median stacking of the available spectra, considering only pixels with no SDSS flag raised. In order to avoid possible biases related to intrinsic dust and differences in signal-to-noise ratio (S/N) within the bin, we excluded spectra in the lowest quartile of the S/N distribution, as well as those galaxies (14 per cent of the entire sample) with $E(B - V) > 0.1$ mag. The colour excess is measured by fitting each SDSS spectrum with a variety of stellar population models, assuming a Cardelli, Clayton & Mathis (1989) extinction law, as detailed in Swindle et al. (2011).

3 IMF-SENSITIVE INDICATORS

The SDSS spectral range allows us to study several IMF-sensitive spectral features, such as the Na I doublet at λλ8183, 8195 Å (Schiavon et al. 1997). This feature is prominent in the atmospheres of low-mass dwarf stars. Therefore, its strength in a stellar population depends quite sensitively on the shape of the IMF at the low-mass end. Over the IMF-sensitive wavelength range (8183–8195 Å), our stacked spectra feature a remarkably high S/N, with an average of ∼400 Å^{-1} for the lowest and highest σ bins, reaching values as high as S/N ∼ 850 Å^{-1} in the stack with velocity dispersion $\sigma \sim 160$ km s^{-1}. We use here a slightly modified version of the NaI8200A index proposed by Vazdekis et al. (2012), defined as Na8190, where the blue passband is measured in the [8137,8147] Å interval (instead of [8164,8173] Å), where the MIUSCAT models are found to give a better match to the data, within ∼0.3 per cent (compared to 1 per cent at $\lambda \sim 8170$ Å). The red and central bandpasses are the same as for the NaI8200A index.

We performed extensive tests to check for possible contamination of the Na8190 feature from sky lines, by combining (1) all galaxies at each λ regardless of the SDSS flag value (2) only flux values not affected by sky absorption (i.e. 1 Å apart from any telluric line) and sky emission and (3) only ETGs at the lowest redshifts in the SPIDER sample ($0.05 \leq z \leq 0.07$), where the Na I doublet is observed in a region free from any significant sky contamination. For all σ bins, the variation of the average Na I flux, using the above three stacking procedures, was found to be smaller than 0.06 per cent, i.e. negligible for our purposes.

In order to increase the robustness of the analysis against possible biases regarding an overabundance of [Na/Fe] in massive galaxies, we also consider two line strengths targeting TiO, a further discriminant with respect to the presence of low-mass stars. We use the TiO1 and TiO2 definitions from the standard Lick system (see e.g. Trager et al. 1998). The TiO2 index has been recently used by Spiniello et al. (2012) to constrain the IMF of a number of early-type gravitational lenses. Fig. 1 shows three of our 18 stacks, in the regions of interest for this work. All spectral energy distributions (SEDs) have been smoothed to a common velocity dispersion of 300 km s^{-1} for a consistent comparison, and were continuum subtracted, using a second-order polynomial. A significant trend is apparent from low- to high-velocity dispersion of all indices. This trend encodes a complex range of variations in the underlying stellar populations, most notably age, metallicity, abundance ratios and IMF.

Note in the Na8190 region (bottom), the centroid of the line shifts bluewards as σ increases. However, because of the asymmetry of

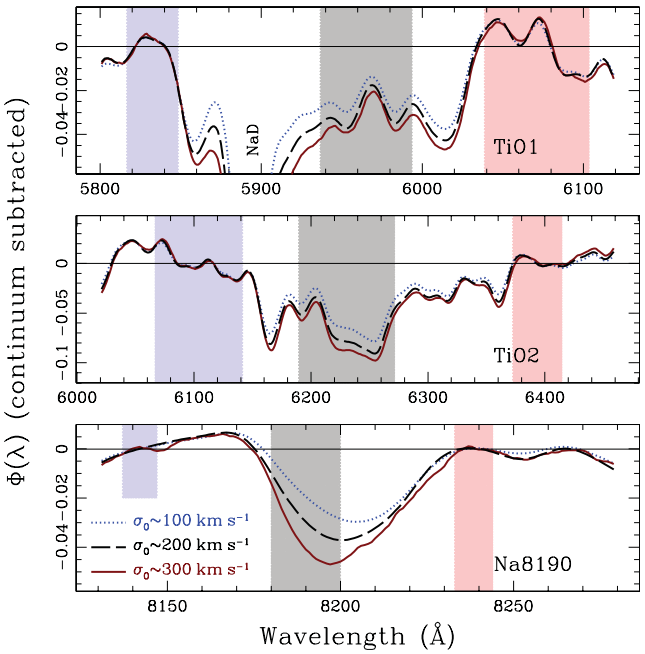

Figure 1. Trend of the three absorption features targeted in this Letter (TiO1, TiO2 and Na8190) with respect to central velocity dispersion, for stacked SDSS spectra of ETGs from the SPIDER sample. The SEDs have been smoothed to a common velocity dispersion of 300 km s^{-1} with the spectral resolution of SDSS, and continuum subtracted with a second-order polynomial. We only show, for clarity, three out of the 18 stacks, spanning the full range of velocity dispersion. The shaded regions mark the positions of the red and blue sidebands, and the central bandpass.

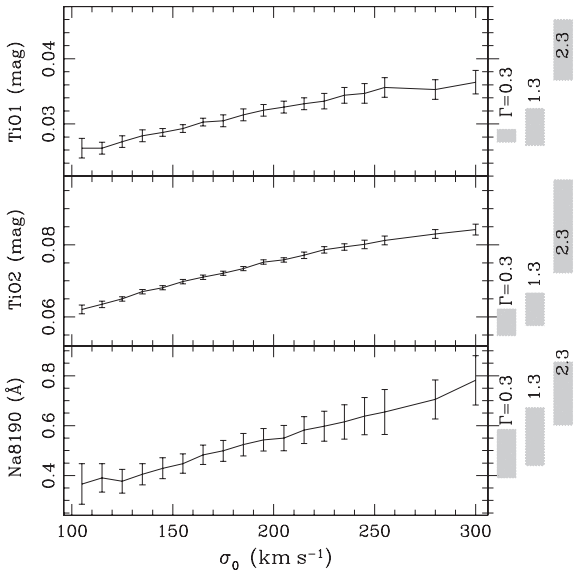

Figure 2. Trend of the equivalent widths of TiO1, TiO2 and Na8190, with respect to velocity dispersion. All measurements are performed on data convolved to a common velocity dispersion of 300 km s^{-1} with the spectral response of SDSS. The error bars give the statistical error from the stacks, at the 3σ level. The shaded regions on the right correspond to model predictions for three choices of IMF unimodal slope, as labelled, spanning a range of ages from 5 to 10 Gyr and metallicity from $\log Z/Z_\odot = -0.4$ to $+0.2$.

the spectral region around the line, more flux would be expected to contribute from the red side of the line, therefore shifting the position of the centroid redwards. This shifting reveals that it is the absorption of Na at 8190 Å – and not other contaminating lines in the vicinity – that changes with respect to the velocity dispersion of the ETG. The two most obvious interpretations of this effect involve either an overabundance of [Na/Fe] (Worthey 1998) or a change in the IMF (Van Dokkum & Conroy 2010). In a forthcoming paper (La Barbera et al., in preparation) we explore in detail the effect of individual overabundances. However, in this Letter, we combine the three line strengths – which rely on different species – to confirm the trend towards a bottom-heavy IMF in massive galaxies.

Fig. 2 shows the line strengths of the stacked SEDs, for the three IMF-sensitive indices. The strengths are corrected to a common broadening of $\sigma_{\rm ref} = 300$ km s^{-1} (in addition to the wavelength-dependent SDSS resolution). A strong correlation of these line strengths with velocity dispersion is evident. We checked that the fixed aperture of the fibres used by SDSS to retrieve spectra did not introduce a bias with respect to size, by comparing the change in line strengths with respect to the angular extent of the effective radius. The variation of the indices, at fixed σ, is around an order of magnitude smaller than the trend shown in Fig. 2. The shaded regions on the right of the figure motivate the methodology followed in this Letter. Each one gives the model predictions for a choice of unimodal IMF slope (labelled), over a range of simple stellar population (SSP) ages and metallicities. The values of all three indices at high-velocity dispersion can only be reconciled with a bottom-heavy IMF. Our methodology – explained below – consists of removing the degeneracies from age and metallicity by combining line strength information with spectral fitting over the optical range.

4 CONSTRAINING THE IMF

We make use of MIUSCAT (Ricciardelli et al. 2012; Vazdekis et al. 2012), the spectrally extended version of the stellar population synthesis models MILES (Vazdekis et al. 2010), in order to map the systematic trend of the TiO1, TiO2 and Na8190 line strengths with respect to IMF slope. These models combine state-of-the art stellar libraries in the optical and NIR windows, creating a set of spectra with a uniform resolution of 2.51 Å throughout the wavelength range 3465–9469 Å. Our data are compared with grids of SSPs, assuming either a unimodal or a bimodal IMF (as defined in Vazdekis et al. 1996), over a stellar mass range 0.1–100 M$_\odot$. For the unimodal case, we adopt the logarithmic slope $\Gamma = x - 1$, where $\mathrm{d}N/\mathrm{d}m \propto m^{-x}$ is the IMF, such that the Salpeter (1955) IMF corresponds to $\Gamma = 1.35$. A bimodal IMF replaces the $M < 0.6\,\mathrm{M}_\odot$ interval by a flat portion and a spline to match the power law at the high-mass end. It gives a closer representation of Kroupa-like IMFs for $\Gamma = 1.3$ (see e.g. fig. 1 of Vazdekis et al. 2003). We use MIUSCAT SSPs spanning a wide range of ages (1–13 Gyr) and metallicities ($-1.0 \leq \log Z/Z_\odot \leq +0.22$), for different values of $\Gamma = \{0.3, 0.8, 1.0, 1.3, 1.5, 1.8, 2.0, 2.3, 2.8, 3.3\}$. In order to obtain an accurate estimate of σ for each stack, we perform spectral fitting with the software STARLIGHT (Cid Fernandes et al. 2005), in the range of 3800–8400 Å. STARLIGHT can be used to extract full star formation histories (see e.g. de la Rosa et al. 2012), but we are only interested here in assessing the robustness of the measured σ with respect to the basis SSPs. We find no significant trend when choosing template SSPs with different IMFs, with a variation $\Delta\sigma \lesssim 1$ km s^{-1}. Furthermore, for each stack, the σ determined by STARLIGHT is consistent, within ~10 per cent, with the median σ of the stacked spectra from SDSS.

We parametrize a stellar population by an age, metallicity and IMF slope. More detailed models will be presented elsewhere (La Barbera et al., in preparation). We note that, according to Thomas, Maraston & Johansson (2011a), both TiO1 and TiO2 are rather insensitive to non-solar abundance ratios. Furthermore, Conroy & van Dokkum (2012a) find an anticorrelation between [α/Fe] and NaI0.82 strength (similar to our Na8190 index). Hence, we do not expect our results, regarding the non-universality of the IMF, to be affected by the well-known overabundance of [α/Fe] in massive galaxies (see e.g. Trager et al. 2000). To confirm this point, we studied two subsamples within the highest σ bin, split with respect to the distribution of [α/Fe] values, constructing low-($\sim+0.1$) and high-($\sim+0.3$) [α/Fe] stacks. The measured TiO1 (mag)/TiO2 (mag)/Na8190 (Å) strengths are $0.0351 \pm 0.0014/0.0860 \pm 0.0010/0.74 \pm 0.07$, for the high [$\alpha$/Fe] subsample, and $0.0352 \pm 0.0015/0.0833 \pm 0.0010/0.77 \pm 0.08$, for the low [$\alpha$/Fe] subsample, which is fully consistent with the original stack, including all values of [α/Fe]: $0.0364 \pm 0.0006/0.0842 \pm 0.0005/0.78 \pm 0.03$.

Our analysis follows a hybrid method, whereby two independent probability distribution functions (PDFs) for age, metallicity and IMF slope are obtained using spectral fitting and line strengths, respectively. For the former, we fit the region 3900–5400 Å, using SSPs from MIUSCAT, after convolving them from the original 2.51 Å resolution, to the fiducial velocity dispersion of 300 km s^{-1}, plus SDSS spectral resolution. A grid of $32 \times 32 \times 10$ models in age, log Z and Γ is used to obtain a PDF, via the likelihood $\mathcal{L} \propto \exp(-\Delta\chi^2/2)$. For each line strength, we also define a second PDF in the same grid. The joint PDF is defined as the product of the corresponding (independent) PDFs. Finally, we marginalize over all parameters but Γ, to obtain the PDF of the IMF slope. Fig. 3 illustrates the constraining power of the different observables, individually, on the age and metallicity of the model SSP. Note that the combined analysis of the hybrid method is acceptable for all three cases (i.e. the joint likelihood does not reduce to the product of mutually unlikely regions of parameter space).

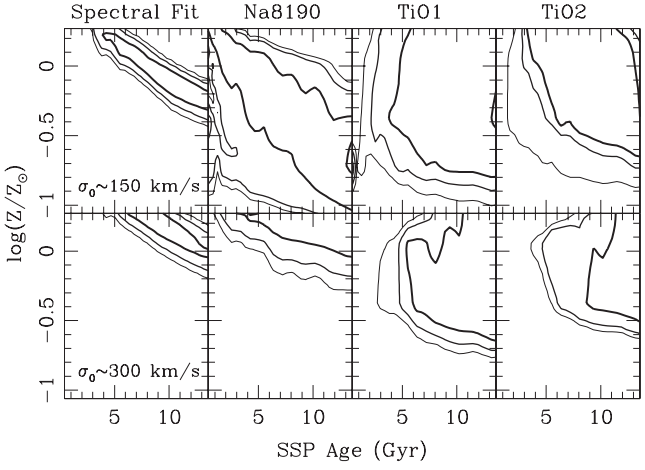

Figure 3. The 68, 95 and 99 per cent confidence levels of the likelihood from individual constraints (from left to right) of spectral fitting, Na8190, TiO1 and TiO2 are shown on the age–metallicity plane for two of the stacks, as labelled by their central velocity dispersion. Bimodal IMFs are used here, although the results for the unimodal case are similar.

5 CONCLUSIONS

Fig. 2 motivates the need to invoke a non-universal IMF when comparing galaxies over a range of velocity dispersions, with an increased contribution from low-mass stars in the most massive galaxies. Fig. 4 presents the best-fitting slope of the IMF, when marginalizing over age and metallicity, as a function of velocity dispersion, given by the probability-weighted estimates using the joint PDF, for three cases, depending on whether TiO1 (filled circles), TiO2 (open squares) or Na8190 (crosses) are used in the analysis. Both unimodal (top) and bimodal (bottom) IMFs are considered. We note that at low-velocity dispersion, the constraint on IMF slope becomes more challenging, as low-mass ETGs feature complex star formation histories (see e.g. de la Rosa et al. 2012), making the SSP approach used here not fully applicable. Therefore, Fig. 4 only shows the range 150–300 km s^{-1}, where the approximation of an SSP is justified. The general trend towards a bottom-heavy IMF is evident in all cases. The result for the joint PDF corresponding to all three indices plus spectral fitting is shown as a grey shaded region – extending over the 68 per cent confidence level – with a black line giving a simple least-squares fit to the data. We emphasize here that accurate values of the IMF slope will require a detailed analysis of abundance ratios (such as e.g. [α/Fe] or [Na/Fe]). The predicted IMF slopes for massive ETGs do not pose a problem to optical–NIR photometry, where the contribution from low-mass stars would be most important. As an example, the MIUSCAT models for a 10-Gyr population at solar metallicity give $V-K=3.04$ for a (bimodal) IMF slope $\Gamma=0.30$ versus $V-K=3.03$ for $\Gamma=2.80$. (A unimodal distribution will give an excess in $V-K$ of $\sim$0.25 mag over a similar range of Γ.) Hence, a variation in the IMF is compatible with the observed $V-K$ colours. Furthermore, $V-K$ colours alone cannot be used to constrain the IMF, a well-known result, that explains why

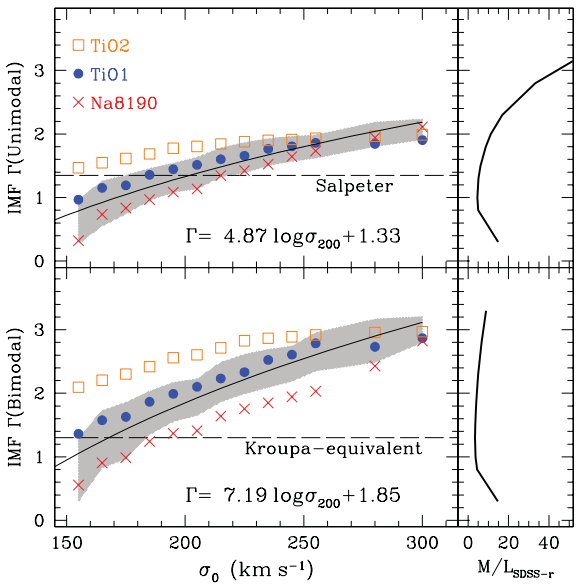

Figure 4. Variation of the IMF slope – unimodal (top) and bimodal (bottom) distributions – against central velocity dispersion. The shaded region corresponds to the 68 per cent confidence level of the joint PDF including spectral fitting and all three line strengths (TiO1, TiO2 and Na8190). The Salpeter (unimodal) and Kroupa equivalent (bimodal) cases are shown as horizontal dashed lines. A least-squares fit to the data is shown for reference (solid line). The rightmost panels give the stellar mass-to-light ratios in the SDSS r band for a 10-Gyr-old population at solar metallicity, illustrating the large variations one could expect depending on the choice of IMF.

constraints on the IMF have remained elusive. The $V-K$ colour of our sample ranges from 3.0 at the lowest velocity dispersion bin, to 3.3 at a velocity dispersion of 300 km s^{-1} (La Barbera et al. 2010).

The rightmost panels of Fig. 4 should serve as a warning to applications of these trends to infer stellar masses. The M/L in the SDSS r band is shown for a typical old, metal-rich population, such as those found in these galaxies. The difference between a unimodal (top) and a bimodal (bottom) IMF is very significant for massive galaxies, whereas the fits for either choice of IMF are equally acceptable. The correlation presented in this Letter is qualitatively consistent with studies based on different methods, involving strong gravitational lensing, or dynamical modelling (see e.g. Treu et al. 2010; Thomas et al. 2011b; Cappellari et al. 2012). Regarding the study of stellar populations, our work is consistent with the trend in Cenarro et al. (2003), based on a spectroscopic analysis of the Ca II triplet region. In addition, the recent photometric analysis of Ricciardelli et al. (2012, see their fig. 16) is compatible with our analysis. Our results are also in agreement with the findings of Van Dokkum & Conroy (2010) and Conroy & Van Dokkum (2012b). We emphasize that our analysis is based on a completely independent stellar library to their work. For instance, in the region around the Na8190 feature, the MIUSCAT models use stellar spectra from the Indo-US library (Valdes et al. 2004), whereas the models of Conroy & van Dokkum (2012a) use the IRTF library (Cushing, Rayner & Vacca 2005; Rayner, Cushing & Vacca 2009). In a forthcoming paper, we will explore in detail different aspects related to the methodology, including the contribution from enhancements of individual elements, non-solar [α/Fe] or composite stellar populations. The large size of our sample – comprising nearly 40 000 ETGs – allowed us to go beyond a simple test of non-universality of the IMF, enabling us to obtain a trend between the IMF slope and velocity dispersion in more detail than previously found. The existing correlation between Γ and velocity dispersion in ETGs suggests a significant transition in the properties of star-forming regions as a function of galaxy mass, an issue with important implications on galaxy formation theories.

ACKNOWLEDGMENTS

IF would like to acknowledge the hospitality of INAF/OAC and the IAC. JF-B acknowledges support from the Ramón y Cajal programme by the Spanish Ministry of Economy and Competitiveness (MINECO). This work has been supported by the Programa Nacional de Astronomía y Astrofísica of MINECO, under grants AYA2010- 21322-C03-01 and AYA2010-21322-C03-02 and by the Generalitat Valenciana (grant PROMETEO-2009-103). This Letter made use of data from the SDSS (http://www.sdss.org/collaboration/credits.html), and also from the UKIRT Infrared Deep Sky Survey (Lawrence et al. 2007).

REFERENCES

Abazajian K. N. et al., 2009, ApJS, 182, 543
Auger M. W., Treu T., Gavazzi R., Bolton A. S., Koopmans L. V. E., Marshall P. J., 2010, ApJ, 721, L163
Bastian N., Covey K. R., Meyer M. R., 2010, ARA&A, 48, 339
Bernardi M., Sheth R. K., Nichol R. C., Schneider D. P., Brinkmann J., 2005, AJ, 129, 61
Birnboim Y., Dekel A., 2003, MNRAS, 345, 349
Brewer B. J. et al., 2012, MNRAS, 422, 3574
Cappellari M. et al., 2006, MNRAS, 366, 1126
Cappellari M. et al., 2012, Nat, 484, 485
Cardelli J. A., Clayton G. C., Mathis J. S., 1989, ApJ, 345, 245
Carter D., Visvanathan N., Pickles A. J., 1986, ApJ, 311, 637
Cenarro A. J., Gorgas J., Vazdekis A., Cardiel N., Peletier R. F., 2003, MNRAS, 339, L12
Chabrier G., 2003, PASP, 115, 763
Cid Fernandes R., Mateus A., Sodré L., Stasinska G., Gomes J. M., 2005, MNRAS, 358, 363
Cohen J. G., 1978, ApJ, 221, 788
Conroy C., van Dokkum P. G., 2012a, ApJ, 747, 69
Conroy C., van Dokkum P. G., 2012b, preprint (arXiv:1205.6473)
Cushing M. C., Rayner J. T., Vacca W. D., 2005, ApJ, 623, 1115
de la Rosa I. G., la Barbera F., Ferreras I., de Carvalho R. R., 2012, MNRAS, 418, L74
De Lucia G., Springel V., White S. D. M., Croton D., Kauffmann G., 2006, MNRAS, 366, 499
Faber S. M., French H. B., 1980, ApJ, 235, 405
Ferreras I., Saha P., Leier D., Courbin F., Falco E. E., 2010, MNRAS, 409, L30
Kroupa P., 2001, MNRAS, 322, 231
La Barbera F., de Carvalho R. R., de La Rosa I. G., Lopes P. A. A., Kohl-Moreira J. L., Capelato H. V., 2010, MNRAS, 408, 1313
Larson R. B., 2005, MNRAS, 359, 211
Lawrence A. et al., 2007, MNRAS, 379, 1599
McKee C. F., Ostriker E. C., 2007, ARA&A, 45, 565
Miller G. E., Scalo J. M., 1979, ApJS, 41, 513
Rayner J. T., Cushing M. C., Vacca W. D., 2009, ApJS, 185, 289
Ricciardelli E., Vazdekis A., Cenarro A. J., Falcón-Barroso J., 2012, MNRAS, 424, 172
Salpeter E. E., 1955, ApJ, 121, 161
Scalo J. M., 1986, Fund. Cosm. Phys., 11, 1
Schiavon R., Barbuy B., Rossi S. C. F., Milone A., 1997, ApJ, 479, 902
Smith R. J., Lucey J. R., Carter D., 2012, preprint (arXiv:1206.4311)
Spiniello C., Trager S. C., Koopmans L. V. E., Chen Y., 2012, ApJ, 753, L32
Swindle R., Gal R. R., La Barbera F., de Carvalho R. R., 2011, AJ, 142, 118
Thomas D., Maraston C., Johansson J., 2011a, MNRAS, 412, 2183
Thomas J. et al., 2011b, MNRAS, 415, 545
Trager S. C., Worthey G., Faber S. M., Burstein D., González J. J., 1998, ApJS, 116, 1
Trager S. C., Faber S. M., Worthey G., González J. J., 2000, AJ, 119, 1645
Treu T., Auger M. W., Koopmans L. V. E., Gavazzi R., Marshall P. J., Bolton A. S., 2010, ApJ, 709, 1195
Valdes F., Gupta R., Rose J. A., Singh H. P., Bell D. J., 2004, ApJS, 152, 251
Van Dokkum P. G., Conroy C., 2010, Nat, 468, 940
Van Dokkum P. G., Conroy C., 2012, preprint (arXiv:1205.6473)
Vazdekis A., Casuso E., Peletier R. F., Beckman J. E., 1996, ApJS, 106, 307
Vazdekis A., Cenarro A. J., Gorgas J., Cardiel N., Peletier R. F., 2003, MNRAS, 340, 1317
Vazdekis A., Sánchez-Bl'azquez P., Falcón-Barroso J., Cenarro A. J., Beasley M. A., Cardiel N., Gorgas J., Peletier R. F., 2010, MNRAS, 404, 1639
Vazdekis A., Ricciardelli E., Cenarro A. J., Rivero-González J. G., Díaz-García L. A., Falcón-Barroso J., 2012, MNRAS, 424, 157
Worthey G., 1998, PASP, 110, 888

This paper has been typeset from a TEX/LATEX file prepared by the author.